

Consensus-based Communication-aware Formation Control for a Dynamical Multi-agent System

Sang Xing

*Department of Mathematics
and Statistics
Portland State University
Portland, OR 97201
sxing@pdx.edu*

Thomas Yang

*Department of Electrical Engineering
and Computer Science
Embry-Riddle Aeronautical University
Daytona Beach, FL 32114
Tianyu.Yang@erau.edu*

Houbing Song

*Department of Electrical Engineering
and Computer Science
Embry-Riddle Aeronautical University
Daytona Beach, FL 32114
h.song@ieee.org*

Abstract—Over the past few decades, unmanned aerial vehicle (UAV) technology has played a significant role in military and civilian applications. To meet the challenges of the future, in addition to improving the functionality and utility of individual aircraft, there is a need to consider how to develop more effective UAV management and organizations. Consequently, among the many developments in UAVs, formation control has become an important concept in recent years. Formation control requires multiple UAVs to adapt to the mission including generate a formation, stay in formation, and change formation. In this paper, we further constrain the formation controller model, not only estimate the desired separation with acceptable accuracy but also ensure a consensus among estimates. Thus, optimizes the overall communication performance of a dynamical multi-agent system.

Index Terms—Unmanned Aerial Vehicles, Multi-agent Systems, Communication-aware, Decentralized, Distributed, Consensus-based, Formation Control

I. INTRODUCTION

Due to the limited equipment can be carried by a single UAV, it is necessary to send out multiple missions to complete a more complex task. A swarm of UAVs operating in formation can disperse equipment, split a complex task into several simple tasks, and assign them to different UAVs in the formation, which will perform the task more efficiently.

Multiple UAVs can carry different equipment and collaborate to accomplish tasks that cannot be accomplished by a single UAV, such as high-precision positioning, multi-angle imaging and theater communication relay. In classical formation control, agents typically perceive their absolute position relative to the global coordinate system, and they actively control the absolute position to achieve their desired formation [1]. Communications between agents are usually assumed to be ideal or within a certain range of communication [2]. In this paper, we adopted ideas from [3], where author Li constructs a new formation controller that uses the communication channel quality, which is measured locally by agents to guide agents into a desired formation. Thus, it also optimizes the quality of communication of the formation system.

Inspired by [4], where the motion of each individual aircraft, better known as agent, is imposed of kinematic unicycle model with constraints on its airspeed and travel direction. We further constrains the communication-aware formation control

to reach a consensus between any pair of connected agents. The formation system is shown in Fig. 1. We imposed a gradient-based control law at the communication layer, which takes the agents' position as input and outputs agents' relative position with respect to its neighboring agents. Consensus controller manages agents' relative positions at the control layer, and outputs the final control of agents with consensus of all agents traveling in the desired direction.

The remainder of the paper are organized as follows. In Section II, we describe the preparatory work in order to understand the formation control process of a dynamical multi-agent system. Section III presents the derivation of interaction model for the communication layer. The final formation controller model is proposed in Section IV. Simulation results are delivered in Section V. Lastly, we concludes the paper in Section VI.

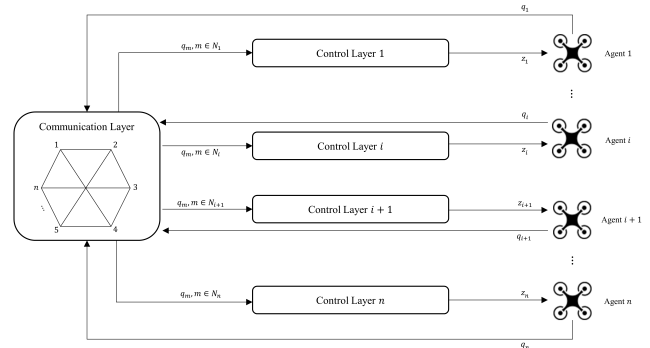


Fig. 1. Schematic diagram of distance-based formation control

II. PRELIMINARIES

A. System Model

Consider the following n single-integrator modeled agents in a two-dimensional space, given by

$$\dot{q}_i = z_i, \quad i = 1, 2, \dots, n, \quad (1)$$

where $q_i, z_i \in \mathbb{R}^2$, $q, z \in \mathbb{R}^{2n}$, and $i \in \mathcal{V}, \mathcal{V} = \{1, 2, \dots, n\}$.

- q_i denotes the *position input* of i -th agent.
- z_i denotes the *control input* of i -th agent.

- The *formation set* is denoted as $q = \{q_1^\top, q_2^\top, \dots, q_n^\top\}^\top$.
- The *control set* is denoted as $z = \{z_1^\top, z_2^\top, \dots, z_n^\top\}^\top$.

B. Graph Theory

A graph G is a pair $(\mathcal{V}, \mathcal{E})$ consisting of a set of vertices $\mathcal{V} = \{1, 2, \dots, n\}$ and a set of ordered pairs of the vertices $\mathcal{E} \subseteq \mathcal{V} \times \mathcal{V}$, called *edges*. I.e., $\mathcal{E} = \{(i, j) \mid i, j \in \mathcal{V}, j \neq i\}$. Here, we assume that there is no self-edge, i.e., $(i, i) \notin \mathcal{E}$.

The graph G is said to be *strongly connected* if there is a path from any node to the other nodes. The graph G is said to be *undirected* if $(i, j) \in \mathcal{E} \Leftrightarrow (j, i) \in \mathcal{E}$. The length of any two vertices in a connected graph is no larger than $n - 1$.

The set of *neighbors* of agent $i \in \mathcal{V}$ is defined as a set $N_i = \{j \in \mathcal{V} : (i, j) \in \mathcal{E}\}$.

C. Rigid Formation

Many researchers have investigated the distributed control of rigid body formation using artificial potential fields [5]. The formation of groups of mobile agents in which all inter-agent distances remain constant is called *rigid* [6]. Many researchers have studied the distributed control of rigid formations by adapting ideas from the theory of graph rigidity. Agents sense relative positions of their neighbors with respect to their own local coordinate systems. To be specific, the relative position vector between agent i and agent j is denoted as $\vec{q}_{ij} = q_i - q_j$ [7] and the relative distance between agent i and agent j is denoted as

$$r_{ij} = \sqrt{(x_i - x_j)^2 + (y_i - y_j)^2} = \|q_i - q_j\|. \quad (2)$$

Let $R > 0$ denote the *communication range* between two agents. In a two-dimensional open ball with radius R (see Fig. 2.), the neighboring set of agent i can be denoted by

$$N_i = \{j \in \mathcal{V} \mid r_{ij} \leq R\}. \quad (3)$$

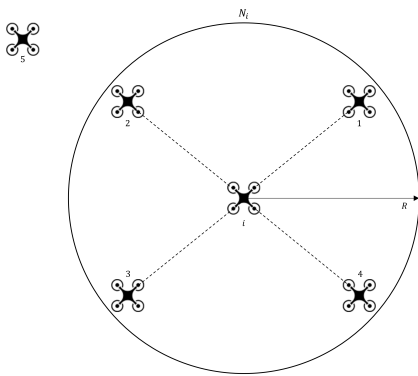


Fig. 2. Agent i and its neighbors in a circle neighborhood

D. Control Gain Matrices

Consider a group of n nonholonomic agents performing formation mission in a two-dimensional plane. We denote $q_i = [x_i, y_i]^\top \in \mathbb{R}^2$ as the position input of agent i in a

common global coordinate frame, and u_i as the consensus control law, that we define as

$$u_i = \sum_{j \in N_i} A_{ij}(q)(q_i - q_j), \quad (4)$$

where $A_{ij} \in \mathbb{R}^{2 \times 2}$ are constant *control gain matrices* constrained in the form

$$A_{ij} = \begin{bmatrix} a_{ij} & b_{ij} \\ -b_{ij} & a_{ij} \end{bmatrix}, \quad a_{ij}, b_{ij} \in \mathbb{R}. \quad (5)$$

Author in [8] showed that the dynamics between q_i and q_j that are expressed in the agents' local coordinate frame is the same as in the case of coordinates expressed in a common global frame. Therefore, while the consensus formation control is distributed and uses the local relative position sensing, the consensus control can be designed and analyzed in a global coordinate frame. The geometric intuition behind the control strategy (4) is explained in [4].

Consequently, the consensus control for all agents in the closed-loop dynamics can be denoted as

$$u = \{u_1^\top, u_2^\top, \dots, u_n^\top\}^\top \in \mathbb{R}^{2n}, \quad (6)$$

where

$$u = Aq, \quad (7)$$

and

$$A = \begin{bmatrix} -\sum_{j=2}^n A_{1j} & A_{12} & \cdots & A_{1n} \\ A_{21} & -\sum_{j=1, j \neq 2}^n A_{2j} & \cdots & A_{2n} \\ \vdots & \vdots & \ddots & \vdots \\ A_{n1} & A_{n2} & \cdots & -\sum_{j=1}^{n-1} A_{nj} \end{bmatrix} \quad (8)$$

is the aggregate state matrix in $\mathbb{R}^{2n \times 2n}$ that consists of A_{ij} 's, and Laplacian matrix structure. For $j \notin N_i$, then $A_{ij} = 0$ in (8). From the Laplacian matrix structure of A , it follows that vectors

$$\begin{aligned} \mathbf{1} &:= [1, 0, 1, 0, \dots, 1, 0]^\top \in \mathbb{R}^{2n} \\ \bar{\mathbf{1}} &:= [0, 1, 0, 1, \dots, 0, 1]^\top \in \mathbb{R}^{2n} \end{aligned} \quad (9)$$

are in the kernel of A .

Let $q^* \in \mathbb{R}^{2n}$ denote the positions of agents in any embedding of the desired formation. Furthermore, let $\bar{q}^* \in \mathbb{R}^{2n}$ denote the coordinates of agent in this embedding when the formation is rotated by 90 degrees around the origin.

It is proven that regardless of the initial condition from which formation starts, the agent will converge to the desired formation [8] through rotations, translations and non-negative scale factors, if A satisfies the following conditions

- Vectors $\mathbf{1}, \bar{\mathbf{1}}, q^*$ and \bar{q}^* are in the kernel of A ,
- Other than the four zero eigenvalues associated with these eigenvectors, the remaining eigenvalues of A have negative real parts.

We then design a stabilizing gain matrix that meets these two conditions listed above. Define

$$B := [q^*, \bar{q}^*, \mathbf{1}, \bar{\mathbf{1}}] \in \mathbb{R}^{2n \times 4}, \quad (10)$$

where $\mathbf{1}, \bar{\mathbf{1}}$ are given in (9). Since B is a set of bases for the kernel of A , we let $USV^\top = B$ be the singular value decomposition (SVD) of B , where

$$U = [\bar{Q}, Q] \in \mathbb{R}^{2n \times 2n}, \quad (11)$$

with $Q \in \mathbb{R}^{2n \times (2n-4)}$ defined as the last $2n - 4$ columns of U . Using Q in (11), we define

$$\bar{A} = Q^\top A Q \in \mathbb{R}^{(2n-4) \times (2n-4)}, \quad (12)$$

to show that matrices A and \bar{A} have the same set of nonzero eigenvalues.

By observation, U is an orthogonal matrix, and $\text{range}(\bar{Q}) = \text{range}(B)$. Therefore \bar{A} is the projection of A onto the orthogonal complement of $\text{range}(B)$. Effectively, the projection (12) eliminates the zero eigenvalues of A allowing us to express the stability of A in terms of \bar{A} .

For an undirected sensing topology, matrix A can be designed to be symmetric. In this case, \bar{A} is symmetric, and its eigenvalues are real and sortable. Thus, A can be computed by solving the optimization problem

$$\begin{aligned} A &= \underset{a_{ij}, b_{ij}}{\text{argmax}} \quad \lambda_{\min}(-\bar{A}) \\ \text{subject to} \quad AB &= 0 \end{aligned} \quad (13)$$

where $\lambda_{\min}(\cdot)$ denote the smallest eigenvalue of a matrix. Since that problem (13) is convex [9], thus it can be formulated even more specifically as the semi-definite programming (SDP) problem

$$\begin{aligned} A &= \underset{a_{ij}, b_{ij}, \gamma}{\text{argmax}} \quad \gamma \\ \text{subject to} \quad \bar{A} + \gamma I &\preceq 0 \\ AB &= 0 \end{aligned} \quad (14)$$

where the first constraint is a linear matrix inequality. Once control gain matrices are computed, they can be transmitted to agents before the mission. A distributed optimization techniques can be used to solve (14) without relying on the complete knowledge of the sensing topology [10]. In recent years, effective algorithms for numerically solving SDPs have been developed and are now available [11]–[13]. The proposed approach for finding stabilizing gain matrix A and consensus control u are summarized in Algorithm 1.

III. COMMUNICATION LAYER

In the communication layer, two different communication models are presented for the signal propagation occurring in the antenna near-field and far-field. In addition, for comprehensive consideration, a communication-aware interaction model is used to illustrate the signal propagation in the near and far-fields of the antenna.

A. Antenna Far-field Propagation

In a mobile ad hoc network, the quality of communication services depends on many unknown parameters besides relative posit, such as multi-path finding, shadowing, noise, and interference [14]. The *outage probability* is introduced as an important wireless channel metric when analyzing the channel

Algorithm 1 Finding A and u

Data: B // Bases of $\ker(A)$
 q // Coordinates of Agents
 u // Consensus Control

Result: Control gain matrix A . Consensus control u .

for $B = (10)$ **do**

$$\begin{aligned} U &= [U, \sim, \sim] = \text{SVD}(B); \\ Q &= U(:, 1:2n-4); \\ \bar{A} &= Q^\top A^* Q; \\ A &= \text{SDP}(\bar{A}) \text{ s.t. satisfies (14)}; \\ u &= A^* q \end{aligned}$$

end

quality. The outage probability is defined as the probability that the instantaneous Signal-to-Noise Ratio (SNR) is below a certain threshold. Thus, it is defined as [15]

$$P_{\text{out}} = 1 - \exp\left(-\alpha(2^\delta - 1)\left(\frac{r}{r_0}\right)^v\right), \quad (15)$$

where α is a system parameter about antenna characteristics, δ is the required application data rate, v is the path loss exponent, that depends on the physical environment, r_0 is a reference distance for the antenna near-field, and r is the distance between a transmitter and a receiver. It is intuitive to see that as r grows, the outage probability $P_{\text{out}} \rightarrow 1$ and, as $r \rightarrow 0$, $P_{\text{out}} \rightarrow 0$ in (15).

Then the *reception probability* of a single input single output (SISO) communication link is defined as

$$P_{\text{recep}} = 1 - P_{\text{out}} = \exp\left(-\alpha(2^\delta - 1)\left(\frac{r}{r_0}\right)^v\right). \quad (16)$$

The reception probability (16) evaluates the probability that the receiver can accurately receive information from the transmitter. The communication channel quality a_{ij} between agent i and agent j in the far field of the antenna is modeled by the reception probability:

$$a_{ij} = \exp\left(-\alpha(2^\delta - 1)\left(\frac{r_{ij}}{r_0}\right)^v\right) = \exp\left(-\beta\left(\frac{r_{ij}}{r_0}\right)^v\right), \quad (17)$$

where $\beta = \alpha(2^\delta - 1)$, and α, δ, v , and r_0 are fixed parameters.

The channel quality (17) is inversely proportional to the inter-agent distance. When the distance between agents is large enough, the reception probability may fall below a certain threshold, which means that the communication between agents becomes unreliable. To some extent, communication range is similar to the reception probability threshold, where inter-agent distances are no longer within the communication range, leading to edge disappearance and message loss. Therefore, we bridge the gap between the communication channel

model and the graph topology model. The set of neighbors of agent i is now defined as

$$N_i = \{j \in \mathcal{V} \mid a_{ij} \geq P_T\}, \quad (18)$$

where P_T is a reception probability threshold. When the reception probability is less than P_T , agents just throw away packets they have received.

B. Antenna Near-field Propagation

The antenna near-field is a region that is close to the antenna. The boundary between antenna near-field and antenna far-field is vaguely defined by the reference distance r_0 [16]. Since the signal propagation in the near-field region of the antenna is quite complex, it is usually difficult to obtain an accurate antenna near-field communication model. For the general tradeoff, we design to use a simple approximate model to capture the signal propagation in the antenna near-field denoted by [15]

$$g_{ij} = \frac{r_{ij}}{\sqrt{r_{ij}^2 + r_0^2}}. \quad (19)$$

It can be concluded from (19) that when $r_{ij} \rightarrow 0$, the channel quality $g_{ij} \rightarrow 0$, which characterizes the interference effect in the antenna near-field; while when r_{ij}/r_0 , $g_{ij} \rightarrow 1$, implying that the interference effect can be ignored in the antenna far-field.

C. Communication-aware Interaction Model

As a matter of fact, the signal scattering effect and the path loss effect are effective in both antenna regions. Therefore, it is necessary to fully consider both two propagations when designing a communication interaction model. Thus, the communication-aware interaction mode is designed as follows [3]:

$$\phi(r_{ij}) = g_{ij} \cdot a_{ij} = \frac{r_{ij}}{\sqrt{r_{ij}^2 + r_0^2}} \cdot \exp\left(-\beta\left(\frac{r_{ij}}{r_0}\right)^v\right). \quad (20)$$

From (20), we want to find distance r_{ij}^* , that brings the optimal inter-agent communication. Due to the path loss effect and signal scattering effect, any value that is larger or smaller than r_{ij}^* distance will result in inadequate communication performance. Therefore, we apply the first-order derivative to (20), to find the maximum of communication performance. We denote the first order derivative of (20) with respect to r_{ij} as

$$\frac{d\phi}{dr_{ij}} = \varphi(r_{ij}), \quad (21)$$

where

$$\varphi(r_{ij}) = \frac{-\beta v (r_{ij})^{v+2} - \beta v r_0^2 (r_{ij})^v + r_0^{v+2}}{\sqrt{(r_{ij}^2 + r_0^2)^3}} \cdot \exp\left(-\beta\left(\frac{r_{ij}}{r_0}\right)^v\right). \quad (22)$$

From (22), we know that both $\sqrt{(r_{ij}^2 + r_0^2)^3}$ and $\exp(-\beta(r_{ij}/r_0)^v)$ are greater than 0 for all $r_{ij} \in [0, \infty)$. So whether $\varphi(r_{ij})$ has a maximum or not is totally determined by the function

$$f(r_{ij}) = -\beta v (r_{ij})^{v+2} - \beta v r_0^2 (r_{ij})^v + r_0^{v+2}. \quad (23)$$

Let $f(r_{ij}) = 0$, the maximum is obtained at

$$r_{ij}^* = \frac{r_0}{(\beta v)^{\frac{1}{v}}}. \quad (24)$$

Moreover,

$$\begin{cases} \varphi(r_{ij}) > 0, & \forall r_{ij} \in [0, r_{ij}^*], \\ \varphi(r_{ij}) = 0, & \forall r_{ij} = r_{ij}^*, \\ \varphi(r_{ij}) < 0, & \forall r_{ij} \in (r_{ij}^*, \infty), \end{cases} \quad (25)$$

which means the communication performance indicator $\phi(r_{ij})$ reaches its maximum performance denoted by ϕ^* at r_{ij}^* given in (24).

IV. CONTROL LAYER

In the control layer, distributed controllers are designed for each mobile agent using the local state and states from the neighbors. Each controller consists of two terms: gradient term and consensus term. By adapting the concept of artificial potential field, the gradient-based controller ensures multi-agents within the communication range R , form and maintain the ideal formation for optimal communication performance. Meanwhile, the consensus controller ensures that eventually all agents will be traveling in one direction over time for a common goal, while still maintaining good communication.

A. Artificial Potential Propagation

An artificial potential function $\psi(r_{ij})$ between agent i and agent j is defined to have the following properties [3]:

- 1) $\psi(r_{ij})$ is a nonnegative function of r_{ij} ,
- 2) $\psi(r_{ij})$ is continuously differentiable,
- 3) $\psi(r_{ij})$ reaches its strict minimum at $r_{ij} = r_\alpha$, i.e., $\psi(r_{ij})$ and $\psi'(r_{ij}) > 0$ for all $r_{ij} \neq r_\alpha$.

The potential function $\psi(r_{ij})$ encrypts a rigid formation with a desired distance r_α . A gradient-based control law is a distributed rigid formation control that can be designed as the negative gradient of its local potential functions

$$\mathcal{G}_i = -\nabla_{q_i} \left[\sum_{j \in N_i} \psi(r_{ij}) \right]. \quad (26)$$

We define a pairwise artificial potential function $\psi(r_{ij})$ by

$$\psi(r_{ij}) = \phi^* - \phi(r_{ij}), \quad \forall (i, j) \in \mathcal{E}. \quad (27)$$

The potential function (27) only evaluates the interaction between neighboring agents. When the topology changes, some edges may be lost or created. Thus we define a new potential function to evaluate the interaction between any pairs of agents regardless of whether they are neighbors or not. The pairwise potential function $\psi_t(r_{ij})$ is defined as

$$\psi_t(r_{ij}) = \begin{cases} \psi(r_{ij}), & \forall (i, j) \in \mathcal{E}, \\ \psi(R) & \text{otherwise.} \end{cases} \quad (28)$$

The potential function $\psi_t(r_{ij})$ keeps fixed for $r_{ij} \geq R$, implying that when edge (i, j) is lost, agents i and agent j will not influence each other any more. Note at the transition point of $r_{ij} = R$, $\psi_t(r_{ij})$ is not necessarily differentiable.

Let $\psi_t(r_{ij})$ be an attractive or repulsive pairwise potential with a global minimum at r_{ij} and a finite cut-off at R . Then, the *collective potential function* of the formation group can be denoted as

$$W(q) = \frac{1}{2} \sum_{i=1}^n \sum_{j=1}^n \psi_t(r_{ij}). \quad (29)$$

When the topology switches, the right-hand side of potential function $W(q)$ may not be smooth.

B. Gradient Controller

Inspired by the ideas of artificial potential fields, the communication-aware formation controller can further optimize the communication performance and maintain the desired formation. It is written as

$$\begin{aligned} \mathcal{G}_i &= -\nabla_{q_i} \left[\sum_{j \in N_i} \psi_t(r_{ij}) \right] \\ &= \nabla_{q_i} \left[\sum_{j \in N_i} \phi(r_{ij}) \right] \\ &= \sum_{j \in N_i} \left[\nabla_{q_i} \phi(r_{ij}) \right] \\ &= \sum_{j \in N_i} \left[\varphi(r_{ij}) \cdot e_{ij} \right], \end{aligned} \quad (30)$$

where $e_{ij} = (q_i - q_j)/r_{ij}$. For a faster convergence, e_{ij} also can be equal to $(q_i - q_j)/\sqrt{1 + kr_{ij}}$, where $k \in (0, 1)$.

C. Unicycle Kinematic Model with Dubins Constraints

One of our objectives is to allow a group of dynamic agents to travel at the same direction. A distributed consensus control scheme is proposed to drive all n agents to a formation in which the agents develops same directional velocity vector over time, and thus optimizes both neighboring communication quality and network coverage. Assume that the airspeed and heading angle of a UAV are adjusted to desired values. We denote $q_i = [x_i, y_i]^\top \in \mathbb{R}^2$ as the position input of agent i in the X - Y frame as illustrated in Fig. 3. The unicycle kinematic model of agent i is:

$$\begin{aligned} \dot{x}_i &= \nu_i \cos(\theta_i) \\ \dot{y}_i &= \nu_i \sin(\theta_i) \\ \dot{\theta}_i &= \omega_i, \end{aligned} \quad (31)$$

The unicycle kinematic model provides a good description of the UAV's motion at a constant altitude [4]. In Fig. 3, $x_i, y_i \in \mathbb{R}$ are coordinates of agent i . The agent's heading vector h_i makes an angle θ_i with respect to x -axis, where $\theta_i \in [0, 2\pi]$. ρ_{ij} represents the line of sight angle between agent i and j with $\rho_{ij} = \arctan 2(q_i - q_j)$. $\nu_i \in \mathbb{R}$ is the linear velocity vector and $\omega_i \in \mathbb{R}$ is respectively the and angular velocity vector of the UAV. Scalars ν_i and ω_i are defined as the projections of the consensus control vector $u_i + cp_i$. u_i is defined in (4) previously. $c > 0$ is a constant desired speed. $p_i \in \mathbb{R}^2$ is the constant unit vector that the i 'th agent should travel along to reach the desired destination.

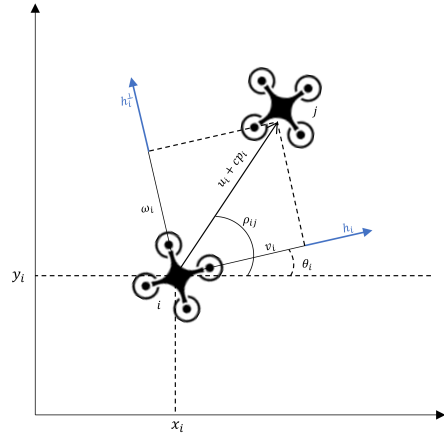


Fig. 3. Close-loop Dynamic with Dubins Constraints

Due to its physical capabilities, the airspeed and heading angle of the UAV are limited. These physical limits can be represented by the constraints

$$\begin{aligned} \nu_{\min} &\leq \nu_i \leq \nu_{\max}, \\ |\omega_i| &\leq \omega_{\max}, \end{aligned} \quad (32)$$

where $\nu_{\max} > \nu_{\min} > 0$ and $\omega_{\max} > 0$ are positive real scalars. Input constraints (32), together with the kinematic model (31), are referred as the Unicycle Kinematic Model with Dubins Constraints. Although this model is well suited for high level path planning and path tracking control design, it does not include aerodynamics, wind effects, disturbances, etc. and is not accurate enough for low level autopilot design.

D. Consensus Controller

To derive an alternative formulation for (31) that is more suitable for the formation control design, we define the heading vector $h_i \in \mathbb{R}^2$ and its perpendicular vector $h_i^\perp \in \mathbb{R}^2$ as

$$h_i := \begin{bmatrix} \cos(\theta_i) \\ \sin(\theta_i) \end{bmatrix}, \quad h_i^\perp := \begin{bmatrix} -\sin(\theta_i) \\ \cos(\theta_i) \end{bmatrix}. \quad (33)$$

The motion of agent i can be expressed by

$$\begin{aligned} \mathcal{C}_i &= h_i \nu_i \\ \dot{h}_i &= h_i^\perp \omega_i, \end{aligned} \quad (34)$$

Let $q = \{q_1^\top, q_2^\top, \dots, q_n^\top\}^\top \in \mathbb{R}^{2n}$ be the aggregate position input vector of all agents, and similarly let $h \in \mathbb{R}^{2n}$, $\nu \in \mathbb{R}^n$, $\omega \in \mathbb{R}^n$ be the aggregate heading, linear velocity, and angular velocity vectors, respectively. Using this notation, the motion of agents can be collectively represented as

$$\begin{aligned} \mathcal{C} &= H\nu \\ \dot{h} &= H^\perp \omega, \end{aligned} \quad (35)$$

where matrices $H, H^\perp \in \mathbb{R}^{2n \times n}$ are defined as

V. SIMULATION AND EVALUATION

$$H = \begin{bmatrix} h_1 & 0 & \cdots & 0 \\ 0 & h_2 & & 0 \\ \vdots & \ddots & \vdots \\ 0 & 0 & \cdots & h_n \end{bmatrix}, H^\perp = \begin{bmatrix} h_1^\perp & 0 & \cdots & 0 \\ 0 & h_2^\perp & & 0 \\ \vdots & \ddots & \vdots \\ 0 & 0 & \cdots & h_n^\perp \end{bmatrix}. \quad (36)$$

Consider a team of UAVs with control (35). We attempt to assign guidance ν and ω to agents so that they autonomously fly towards the same desired destination.

The proposed consensus control strategy for a multi-agent system is as follows. Each agent computes the control vector $u_i + cp_i$. The projections of this vector along the heading direction h_i and its perpendicular vector h_i^\perp are then calculated and used as the linear and angular velocity vectors, respectively. Specifically, the linear and angular velocity controls are given by

$$\begin{aligned} \nu_i &= h_i^\top (u + cp_i) \cos(\rho_{ij} - \theta_i) \\ \omega_i &= h_i^{\perp\top} (u + cp_i) \sin(\rho_{ij} - \theta_i) \end{aligned} \quad (37)$$

as illustrated in Fig. 3.

The control for all agents can be expressed collectively in the vector form as

$$\begin{aligned} \nu &= H^\top (u + cp) \cos(\rho - \theta) \\ \omega &= H^{\perp\top} (u + cp) \sin(\rho - \theta) \end{aligned} \quad (38)$$

where H and H^\perp are defined in (36). Under the proposed control, the consensus dynamics are given by replacing (37) in (34) as

$$\begin{aligned} \mathcal{C}_i &= h_i h_i^\top (u + cp_i) \cos(\rho_{ij} - \theta_i) \\ \dot{h}_i &= h_i^\perp h_i^{\perp\top} (u + cp_i) \sin(\rho_{ij} - \theta_i), \end{aligned} \quad (39)$$

and collectively

$$\begin{aligned} \mathcal{C} &= HH^\top (u + cp) \cos(\rho - \theta) \\ \dot{h} &= H^\perp H^{\perp\top} (u + cp) \sin(\rho - \theta). \end{aligned} \quad (40)$$

E. Constrained Formation Controller

Finally, the dynamics of this multi-agent system thus can be expressed by the sum of gradient-based control and consensus control where

$$\begin{aligned} \dot{q}_i &= z_i \\ &= \sum_{j \in N_i} \underbrace{[\varphi(r_{ij}) \cdot e_{ij}]}_{\text{gradient-based term}} + \sum_{j \in N_i} \underbrace{[A_{ij}(q)(q_i - q_j)]}_{\text{consensus term}} \\ &= \sum_{j \in N_i} \underbrace{[\varphi(r_{ij}) \cdot e_{ij}]}_{\text{gradient-based term}} + \sum_{j \in N_i} \underbrace{[h_i h_i^\top (u + cp_i) \cos(\rho_{ij} - \theta_i)]}_{\text{consensus term}} \\ &= \mathcal{G}_i + \mathcal{C}_i. \end{aligned} \quad (41)$$

In this section, we provide a few simulation examples to illustrate our proposed formation control method. The simulation of our proposed method is implemented in the following table of simulation parameters. The position input of agents are chosen randomly in a static environment. The desired formation is implemented using Algorithm 2.

TABLE I
SIMULATION PARAMETERS

Parameter	Value
α	1×10^{-5}
δ	2
v	3
r_0	5
P_T	94%

Algorithm 2 Proposed Formation Control Algorithm

Data: $itr \leftarrow 1000$ // Number of Iterations
 $n \leftarrow 8$ // Number of Agents
 $J \leftarrow N_i$ // Number of Neighbors
 a_{ij} // Communication Near-field Model
 $P_T \leftarrow 0.94$ // Reception Threshold
 φ_{ij} // Interaction Model
 \mathcal{G}_i // Gradient-term Controller
 \mathcal{C}_i // Consensus-term Controller
 \dot{q} // Dynamics of Multi-agent System

Result: Desired Swarm Formation Control (see Fig. 4.)

```

for 1 :  $itr$  do
  for 1 :  $n$  do
    for  $J = N_i ; a_{ij} = (17)$  do
      if  $a_{ij} \geq P_T$  then
        |  $\varphi(r_{ij}) = (22);$ 
      else
        |  $\varphi(r_{ij}) = 0;$ 
      end
    end
  end
   $\mathcal{G}_i = (30);$ 
   $\mathcal{C}_i = (39);$ 
   $\dot{q} = \mathcal{G}_i + \mathcal{C}_i$ 
end

```

Consider a group of 8 agents evolving in a practical communication environment with the given communication setting. The initial topology of 8 agents in the given communication environment is shown in Fig. 5(a), where the initial positions of 8 agents are given by $x_1 = [-5, -14]^\top$, $x_2 = [-5, -19]^\top$, $x_3 = [0, 0]^\top$, $x_4 = [20, 21]^\top$, $x_5 = [35, 41]^\top$, $x_6 = [68, 0]^\top$, $x_7 = [72, 13]^\top$, $x_8 = [72, -18]^\top$.

The circular node represents each agent. The blue line represents the initial communication link. The red arrows represent the directional vectors of each agent.

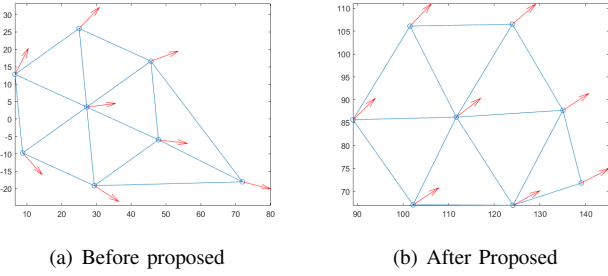


Fig. 4. Multi-agent system before and after our proposed formation control algorithm

Fig. 4(a) shows the result of 8 agents before our proposed control (41). Fig. 4(b) shows that after our proposed implementation, all the agents are able to walk along the same direction and approach to each other in a desired formation.

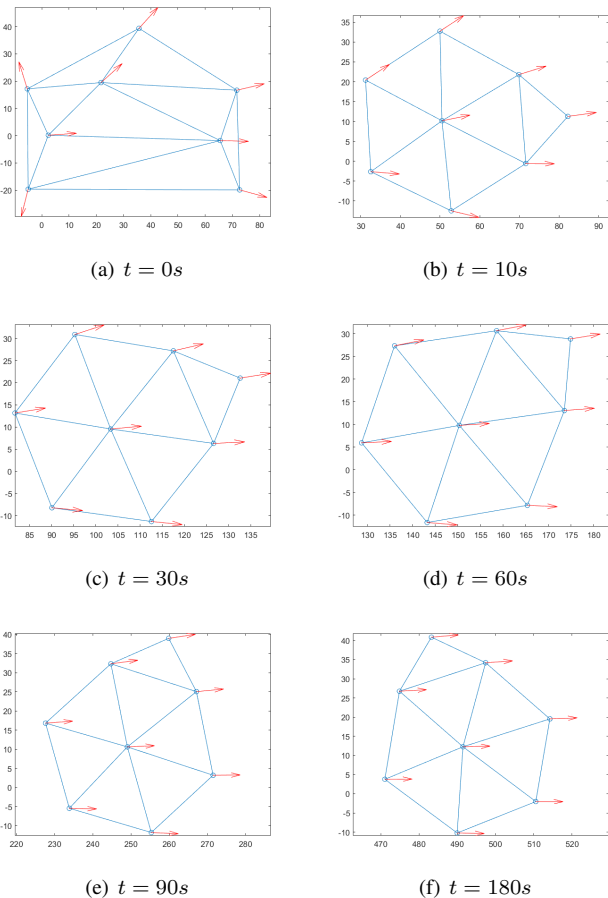


Fig. 5. Simulation of 8 UAVs starting from random initial pose and achieving an optimal formation while traveling along toward the positive x -axis.

Fig. 5 provides another simulation result where all agents eventually reach a consensus and travel in the positive direction of the x -axis over time.

A comprehensive performance index is introduced here to show that the optimal communication performance is achieved at a tradeoff distance between agents. The average neighboring distance r_n and average communication performance J_n are defined as

$$r_n = \frac{\sum_{i=1}^n \sum_{j \in N_i} r_{ij}}{2n|N_i|}, \quad (42)$$

$$J_n = \frac{\sum_{i=1}^n \sum_{j \in N_i} \phi(r_{ij})}{2n|N_i|}, \quad (43)$$

where $|N_i|$ represents the size of neighbors of agent i .

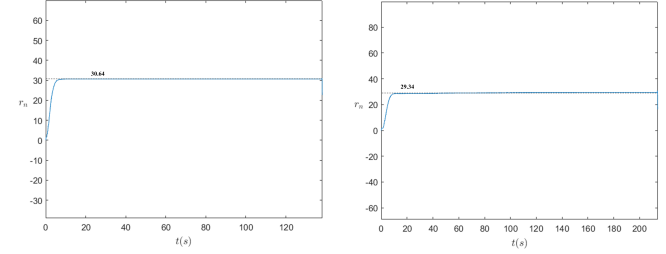


Fig. 6. Average Neighboring Distance Indicator

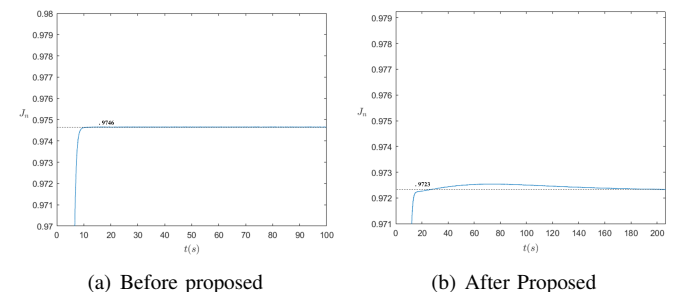


Fig. 7. Average Communication Performance Indicator

Fig. 6 showed that our proposed method was able to bring agents closer to each other. Fig. 7 shows that the communication performance of our proposed method is slightly lower compared to the original control strategy.

VI. CONCLUSION

In this paper, we study a new distributed control strategy for multi-agent systems, where formation control with communication constraints were used to achieve desired formations with optimal communication performance. Consensus control is also successfully enforced for a set of agents traveling in the same directions toward a desired destination. We were also able to maintain a similar average neighboring distance and achieve sufficient average communication performance.

ACKNOWLEDGMENT

This research was supported by the National Science Foundation under Grant No. 2150213.

REFERENCES

- [1] K.-K. Oh, M.-C. Park, and H.-S. Ahn, "A survey of multi-agent formation control," *Automatica*, vol. 53, pp. 424-440, Mar. 2015.
- [2] Y. Yan and Y. Mostofi, "Robotic Router Formation in Realistic Communication Environments," in *IEEE Transactions on Robotics*, vol. 28, no. 4, pp. 810-827, Aug. 2012.
- [3] H. Li, J. Peng, W. Liu, K. Gao, and Z. Huang, "A novel communication-aware formation control strategy for dynamical multi-agent systems," *Journal of the Franklin Institute*, vol. 352, no. 9, pp. 3701-3715, Sep. 2015.
- [4] K. Fathian, T. H. Summers, and N. R. Gans, "Distributed formation control and navigation of fixed-wing UAVs at constant altitude," in *2018 International Conference on Unmanned Aircraft Systems (ICUAS)*, 2018.
- [5] A. Durniak, "Welcome to IEEE Xplore," *IEEE power eng. rev.*, vol. 20, no. 11, p. 12, 2000.
- [6] J. Baillieul and P. J. Antsaklis, "Control and communication challenges in networked real-time systems," *Proc. IEEE Inst. Electr. Electron. Eng.*, vol. 95, no. 1, pp. 9-28, 2007.
- [7] R. Olfati-Saber, "Flocking for multi-agent dynamic systems: algorithms and theory," *IEEE Transactions on Automatic Control*, vol. 51, no. 3, pp. 401-420, Mar. 2006.
- [8] K. Fathian, D. I. Rachinskii, T. H. Summers, M. W. Spong, and N. R. Gans, "Distributed formation control under arbitrarily changing topology," in *2017 American Control Conference (ACC)*, 2017.
- [9] S. Boyd, "Convex optimization of graph Laplacian eigenvalues," in *Proceedings of the International Congress of Mathematicians Madrid, August 22-30, 2006, Zuerich, Switzerland: European Mathematical Society Publishing House*, 2009, pp. 1311-1319.
- [10] Z. Lin, L. Wang, Z. Chen, M. Fu, and Z. Han, "Necessary and sufficient graphical conditions for affine formation control," *IEEE Trans. Automat. Contr.*, vol. 61, no. 10, pp. 2877-2891, 2016.
- [11] Tütüncü, H. Reha, K. C. Toh, and M. J. Todd, "Solving semidefinite-quadratic-linear programs using SDPT3," *Math. Program.*, vol. 95, no. 2, pp. 189-217, 2003.
- [12] M. J. Todd, K. C. Toh, and R. H. Tütüncü, "On the Nesterov-Todd Direction in Semidefinite Programming," *SIAM J. Optim.*, vol. 8, no. 3, pp. 769-796, 1998.
- [13] K. C. Toh, M. J. Todd, and R. H. Tütüncü, "SDPT3 — A Matlab software package for semidefinite programming, Version 1.3," *Optim. Methods Softw.*, vol. 11, no. 1-4, pp. 545-581, 1999.
- [14] C. Li, Z. Qu, and M. A. Weitnauer, "Distributed extremum seeking and formation control for nonholonomic mobile network," *Systems Control Letters*, vol. 75, pp. 27-34, Jan. 2015.
- [15] A. Goldsmith, *Wireless Communications*. Cambridge, England: Cambridge University Press, 2012.
- [16] H. Li, J. Peng, X. Zhang, and Z. Huang, "Flocking of Mobile Agents Using a New Interaction Model: A Cyber-Physical Perspective," *IEEE Access*, vol. 5, pp. 2665-2675, 2017.